

Non-enzymatic electrochemical sensors for the detection of H₂O₂ based on Mn₃O₄ octahedron submicrostructures

Liang Wang¹, Kong-Lin Wu¹, Bin-Bin Jiang², Zai-Xian Zhang¹, Xiang-Zi Li³, Bei Zhang¹, Ju Lv¹, Jian Suan¹, Chao Dong¹

¹College of Chemistry and Materials Science, The Key Laboratory of Functional Molecular Solids, Ministry of Education, Anhui Laboratory of Molecular-Based Materials, Anhui Normal University, Wuhu 241000, People's Republic of China

²School of Chemical and Engineering, Anhui University of Technology, Maanshan 243002, People's Republic of China

³Department of Chemistry, Wannan Medical College, Wuhu 241002, People's Republic of China

E-mail: konglin@mail.ahnu.edu.cn

Published in Micro & Nano Letters; Received on 9th March 2014; Revised on 26th August 2014; Accepted on 9th September 2014

In this reported work, Mn₃O₄ octahedron submicrostructures (Mn₃O₄ OSMs) were obtained through a facile solvothermal method in mixed solvent. The authors have modified a glassy carbon electrode (GCE) with Mn₃O₄ OSMs and Nafion to obtain a sensing platform (Mn₃O₄ OSMs/Nafion/GCE) for the non-enzymatic detection of H₂O₂. The resulting Mn₃O₄ OSMs/Nafion/GCE exhibited good electrochemical catalytic activity towards the reduction of H₂O₂ in a phosphate buffered solution (0.1 M, pH = 7.0). The linear detection range was estimated to be in the range from 5 µM to 17 mM ($R = 0.9998$), and the detection limit was estimated to be 1.5 µM at $S/N = 3$. Real sample analyses show that the sensor developed in this work could be efficiently used for the determination of H₂O₂.

1. Introduction: H₂O₂, an important intermediate, plays a significant role in the fields of biomedicine, environmental science and the food industry [1]. Therefore, many detection methods have been developed, such as the fluorescence, spectrometry, titrimetry, electrochemistry methods and so on. The direct electrochemistry method is an attractive new method that has become a very interesting subject because of its low detection limit, high sensitivity and high selectivity. Various materials have been successfully applied in the construction of non-enzymatic sensors, such as metals [2], alloys [3], nanocomposites based on carbon nanotubes [4–6] or graphene [7–9] and especially metal oxides [10]. As an important functional metal oxide, manganese oxides (such as MnO [11], MnO₂ [12–17], Mn₂O₃ [18] etc.) have attracted considerable attention in electrocatalysis or biosensors. In general, Mn₃O₄ is known to be an active catalyst for several oxidation and reduction reactions [19, 20], especially for biosensors [21–23]. For example, Gao and co-workers [21] reported that several manganese-based nanostructures have been prepared through the redox reactions between KMnO₄ and sodium carboxymethyl cellulose. The direct electrochemical behaviour of cytochrome *c* immobilised on an Mn₃O₄-modified glassy carbon electrode (GCE) showed that the Mn₃O₄ nanoparticles could promote direct electron transfer between cytochrome *c* and the electrode [21]. Reza *et al.* [22] reported that highly sensitive Mn₃O₄ nanocomposite was developed for biosensor applications. Furthermore, Kim and co-workers [23] reported a novel composite material of hierarchically structured Mn₃O₄ grown on three-dimensional (3D) graphene foam (3DGF), and this hierarchical Mn₃O₄/3DGF composite was fabricated as a flexible and freestanding biosensor for the non-enzymatic determination of glucose and H₂O₂ in alkaline electrolyte. However, the study of electrochemical/biosensing properties based on Mn₃O₄ materials is very limited. To the best of our knowledge, no reports exist regarding the application of Mn₃O₄ OSMs in enzyme-free amperometric H₂O₂ biosensors.

Herein, we report a solvothermal technique to synthesise Mn₃O₄ OSMs in mixed solvent. We constructed a non-enzymatic H₂O₂ sensor based on an Mn₃O₄ OSMs-modified GCE (Mn₃O₄ OSMs/GCE). The electrochemical catalytic activities of the Mn₃O₄

OSMs/GCE towards H₂O₂ were studied. The properties of the sensors based on these electrodes, such as sensitivity, selectivity and the detection limit in the H₂O₂ detection were investigated. Moreover, the potential use of the Mn₃O₄ OSMs/Nafion/GCE for analysis application in milk was carried out.

2. Experimental

2.1. Synthesis of Mn₃O₄ OSMs: The Mn₃O₄ OSMs with yields of ~65% (wt%) were synthesised via a solvothermal technique in mixed solvent. In a typical synthesis, 3 mmol MnCl₂·4H₂O, 2 mmol urea and 5 mmol polyvinylpyrrolidone (PVP) were dissolved in mixed solvent (20 ml H₂O and 20 ml 1, 2-propanediol) under magnetic stirring. After 30 min stirring, the mixture was transferred and sealed in a 60 ml Teflon-lined autoclave, heated at 120°C for 12 h and finally cooled to room temperature. The precipitate was collected by centrifugation (10 000 rpm, 4 min), washed alternately with deionised water and ethanol four times and several times under ultrasonic conditions and then dried in a vacuum oven at 60°C for 10 h.

2.2. Characterisation: The structural information and purity of the samples were collected by X-ray powder diffraction (XRD) measurements that were carried out on a Shimadzu XRD-6000 X-ray diffractometer (Cu K α radiation, $\lambda = 1.5406$ Å) with 2θ value from 10° to 70° at a scanning rate of 0.2°/s. The operation voltage and current were kept at 40 kV and 30 mA, respectively. The morphologies of the samples were studied by scanning electron microscopy (SEM, Hitachi S-4800, Japan) and transmission electron microscopy (TEM, FEI Tecnai G² 20, 200 kV, Holand).

2.3. Electrochemical measurement: Electrochemical measurements were performed on a model CHI 660C electrochemical workstation (Chen Hua Instruments Co. Ltd, Shanghai, China) controlled by a personal computer. 10 mg Mn₃O₄ OSMs were dispersed in 10 ml of dimethylformamide containing 0.05% Nafion, then 5 µl of the corresponding suspension was coated on the glass carbon electrode (GCE) and dried in air to fabricate the Mn₃O₄ OSMs/Nafion/GCE. The coiled Pt wire electrode and the saturated calomel electrode were applied as the reference auxiliary and the

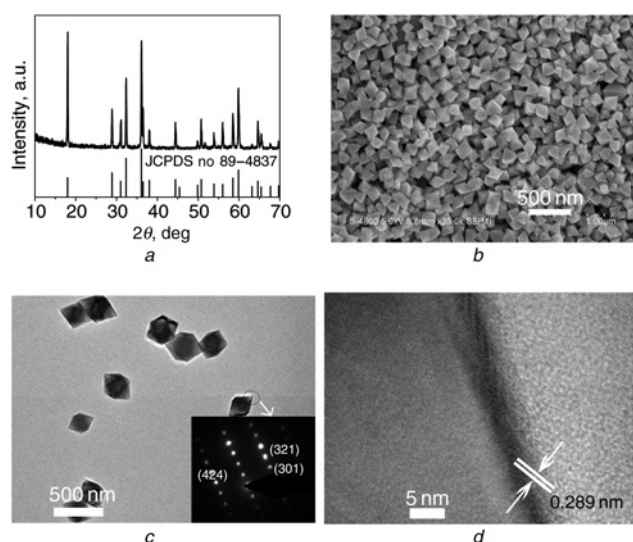


Figure 1 Characterisation of the as-obtained Mn_3O_4 OSMs
 a XRD pattern
 b SEM image
 c TEM image (inset is the SAED pattern)
 d HRTEM image

auxiliary electrode, respectively, and the Mn_3O_4 OSMs/Nafion/GCE as the working electrode was put into a cell with 10 ml of 0.1 M phosphate buffered solution (PBS, pH = 7.0) to check the electro reduction ability to H_2O_2 . The cyclic voltammetry (CV) scanning rate was set to be 50 mV s^{-1} . The amperometric curves were obtained after adding a certain concentration of H_2O_2 with the solution stirred constantly.

3. Results and discussion

3.1. Characterisation of Mn_3O_4 crystals: Fig. 1a shows the typical XRD pattern of the products prepared by the solvothermal method. All the diffraction peaks can be indexed to the tetragonal hausmannite structure of Mn_3O_4 (JCPDS No. 89-4837), and the sharpness of the peaks implies the high crystalline quality of the as-obtained sample. No peaks of impurities can be detected, indicating that pure Mn_3O_4 crystals have been prepared through the reaction of $\text{MnCl}_2 \cdot 4\text{H}_2\text{O}$ and urea. The morphology of the Mn_3O_4 crystals was characterised by SEM and TEM. The low-magnification SEM image (Fig. 1b) reveals that the sample is composed of uniform Mn_3O_4 OSMs. Fig. 1c shows the TEM image of the as-obtained Mn_3O_4 OSMs. It can be clearly seen that the products contain a uniform octahedral morphology, which is consistent with the results of the SEM (Fig. 1b). Lattice fringes can be observed with high-resolution TEM (HRTEM) imaging (Fig. 1d). The interplanar spacings corresponding to the (200) plane of the tetragonal phase of Mn_3O_4 was approximately about 0.289 nm. The selected area electron diffraction (SAED) pattern inset in Fig. 1c reveals the single crystalline nature of the Mn_3O_4 samples. In the absence of PVP, the shapes of products with imperfect OSMs, and some particles and rods were obtained

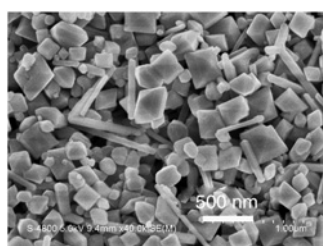


Figure 2 SEM image of Mn_3O_4 crystals obtained in the absence of PVP

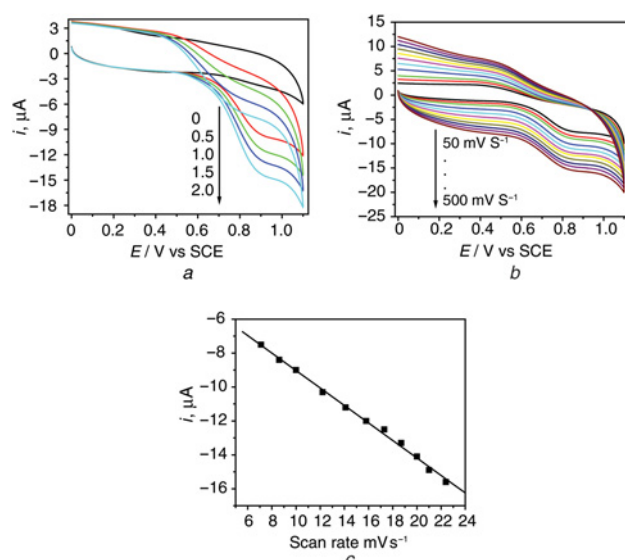


Figure 3 CVs and plot of peak current against the potential scan rate of Mn_3O_4 OSMs/Nafion/GCE
 a CVs at a scan rate of 50 mV s^{-1} with 0, 0.5, 1, 1.5 and 2 mM of H_2O_2
 b CVs at different scan rates with 0.5 mM of H_2O_2
 c Plot of peak current against the different scan rates with 0.5 mM of H_2O_2

(Fig. 2). So, in our synthesis process, the surfactant of PVP was needed to control the morphology of the Mn_3O_4 OSMs.

3.2. Electrochemical behaviour of Mn_3O_4 OSMs/Nafion/GCE: To evaluate the Mn_3O_4 OSMs as an electrode material for practical application, the obtained Mn_3O_4 OSMs were immobilised on a GCE and applied in an amperometric H_2O_2 biosensor. The electrocatalytic activities of the Mn_3O_4 OSMs/Nafion/GCE towards the electro reduction of H_2O_2 with different concentrations in phosphate buffered saline (PBS, 0.1 M, pH = 7.0) solution at 50 mV s^{-1} were investigated using CV. As shown in Fig. 3a, the current density of the electrocatalytic peaks enhanced with increasing the concentration of H_2O_2 , which demonstrates the high stability of the Mn_3O_4 OSMs/Nafion/GCE to the reduction of H_2O_2 in 0.1 M PBS (pH = 7.0), pointing to its potential for developing Mn_3O_4 OSMs/Nafion/GCE as a non-enzymatic H_2O_2 sensor. The effects of different scan rates on the reduction of H_2O_2 at Mn_3O_4 OSMs/Nafion/GCE in 0.1 M PBS was also investigated by CV (Fig. 3b). As shown in Fig. 3c, a good linearity between scan rate and peak current was obtained in the range of $50\text{--}500 \text{ mV s}^{-1}$, and the linear regression equation, $I = -3.873 - 0.516v^{1/2}$, with the correlation coefficient (R) of 0.998. The result indicates that the electrochemical kinetics is controlled by the diffusion of H_2O_2 .

3.3. Optimisation for H_2O_2 sensing: It is well known that the detection potential strongly affects the amperometric response of a

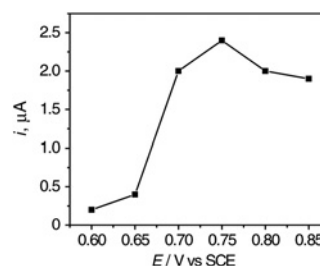


Figure 4 Effect of applied potential on peak current to 0.5 mM H_2O_2 for Mn_3O_4 OSMs/Nafion/GCE

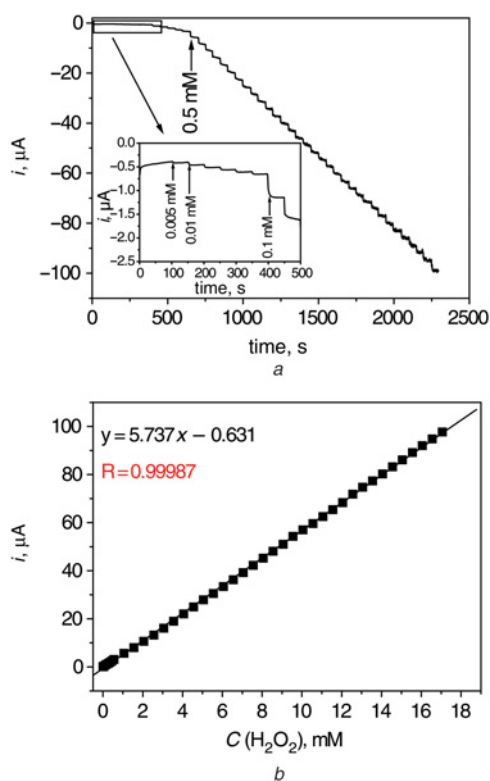


Figure 5 Amperometric response of Mn_3O_4 OSMs/Nafion/GCE to H_2O_2 in 0.1 M PBS (pH = 7.0), the scan rate was 50 mV s^{-1}
a Successive amperometric response to H_2O_2
b Calibration plot for amperometric determination of H_2O_2

biosensor. We have systematically investigated the impact of detection potential on the amperometric response of Mn_3O_4 OSMs/Nafion/GCE to H_2O_2 . Fig. 4 shows the peak currents for applied potentials from +0.6 to +0.85 V after the addition of 0.5 mM H_2O_2 to 0.1 M PBS (pH=7.0). The peak current reached a maximum for an applied potential of +0.75 V. Thus, +0.75 V was chosen as the optimal potential for amperometric H_2O_2 sensing.

3.4. Amperometric response of the Mn_3O_4 OSMs/Nafion/GCE towards H_2O_2 : Fig. 5a shows the typical current-time dynamic response of the Mn_3O_4 OSMs/Nafion/GCE towards H_2O_2 . The modified electrode responded quickly to the change of H_2O_2 concentration. When an aliquot of H_2O_2 was added into the buffer solution, the reduction current rose steeply until a stable value was reached within a short period of about 4 s. It indicates a fast, sensitive response to H_2O_2 , which should be attributed to the fact that Mn_3O_4 OSMs can promote direct electron transfer between H_2O_2 and the electrode [23]. From the amperometric curve for H_2O_2 in Fig. 5b, the linear relationship between the reduction current and the H_2O_2 concentration was obtained for a concentration ranging from 0.005 to 17 mM, M and the

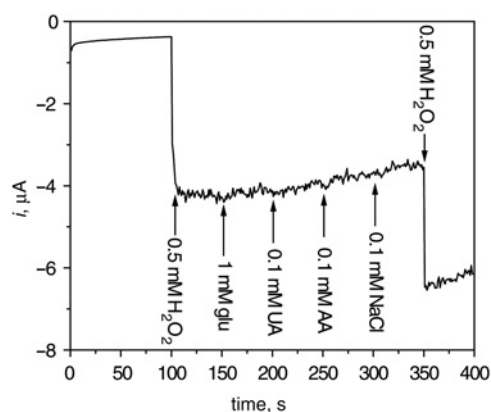


Figure 6 Amperometric response of the Mn_3O_4 OSMs/Nafion/GCE with successive addition of 0.5 mM H_2O_2 , 1 mM glu, 0.1 mM UA, 0.1 mM AA, 0.1 mM NaCl and 0.5 mM H_2O_2 in PBS solution (pH = 7.0)

correlation coefficient of the line was $R=0.998$. The detection limit of H_2O_2 using an Mn_3O_4 OSMs/Nafion/GCE was found to be $1.5 \mu\text{M}$ ($S/N=3$), which was lower than that of Pt-DENs ($2.5 \mu\text{M}$) [5], MWNTs/Cu-Ag ($2.82 \mu\text{M}$) [6], Cu-Ag/rGO NC ($12 \mu\text{M}$) [8], β - MnO_2 nanorods ($2.45 \mu\text{M}$) [17], AgNP/PQ11/graphene ($28 \mu\text{M}$) [24] and PQ11AgNPs ($33 \mu\text{M}$) [25]. The Mn_3O_4 OSMs/Nafion/GCE exhibits a wider linear detection range (0.005–17 mM) than that of the Cu-Ag/rGO NC (0.05–1.1 mM) [8], Mn_3O_4 /3DGF composite (0.002–6.5 mM) [23] and GO/ MnO_2 (0.005–0.6 mM) [26] modified GCE. For comparison, the performances of the H_2O_2 sensors reported in the literature have been listed in Table 1.

3.5. Repeatability, stability and anti-interference property of the Mn_3O_4 OSMs/Nafion/GCE: The repeatability of Mn_3O_4 OSMs/Nafion/GCE was examined by measurement of the amperometric

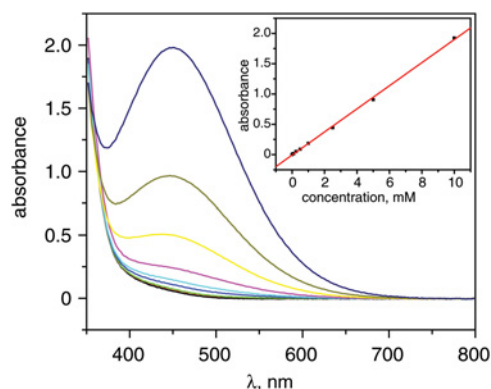


Figure 7 Absorbance curves for vanadate solution with different H_2O_2 concentrations (inset is the linear curve)

Table 1 Comparison of the performances of the proposed Mn_3O_4 OSMs/Nafion sensor with other published non-enzymatic H_2O_2 sensors

Electrode materials	Response time, s	Linear range, mM	Detection limit, μM	References
Mn_3O_4 OSMs	4	0.005–17	1.5	this work
Pt-DENs	5	–	2.5	[5]
MWNTs/Cu-Ag	–	0.002–0.42	2.82	[6]
Cu-Ag/rGO NC	2	0.05–1.1	12	[8]
β - MnO_2 nanorods	5	0.00245–42.85	2.45	[17]
Mn_3O_4 /3DGF	3	0.002–6.5	1.0	[23]
GO/ MnO_2	5	0.005–0.6	0.08	[26]

Table 2 Concentration of H₂O₂ determined by spectrophotometric method and electrochemical method in samples taken from different H₂O₂ concentrations of 3.0 and 4.0 mM, respectively

Sample	Added, mM	Spectrophotometric method			Electrochemical method		
		Found, mM	Recovery, %	R.S.D., %	Found, mM	Recovery, %	R.S.D., %
1	3.0	2.89	96.2	0.59	2.90	96.9	2.45
2	4.0	3.91	97.7	0.5	4.15	103.7	3.17

Table 3 Determination of H₂O₂ concentration in the milk sample ($n = 4$) by electrochemical method

Sample	Add, mM	Found, mM	Recovery, %	R.S.D., %, $n = 4$
1	5	5.21	104.2	4.67
2	6	6.15	102.5	5.17
3	7	6.65	95.0	3.76

response to 0.5 mM H₂O₂. The relative standard deviation for ten successive amperometric determinations yielded an RSD of 3.5%, indicating a good repeatability. The stability of the modified electrode was evaluated for 48 h by storing at 4°C. The response current maintained 95.2% of its initial response, demonstrating a good stability, while the Mn₃O₄ OSMs/Nafion/GCE could retain 85% of the pristine current value. The anti-interference property and the stability of Mn₃O₄ OSMs/Nafion/GCE are crucial for the development of a non-enzymatic electrochemical biosensor, as the species such as glucose (glu), uric acid (UA), ascorbic acid (AA) and NaCl easily influence the electrochemical response for H₂O₂ which needs to be examined at the Mn₃O₄ OSMs/Nafion/GCE. In this study, the interference experiment was carried out by adding the interfering species into 0.5 mM H₂O₂ in 0.1 M PBS (pH = 7.0). As shown in Fig. 6, no significant signals can be observed for the interfering species when the well-defined H₂O₂ reduction currents were obtained. After the injection of 0.5 mM H₂O₂, a weak drift from 6.47 to 5.94 μ A (Fig. 5, ~50 s) was observed. However, the error is still lower than ~5%, and shows to weakly influence the sensor in potential applications.

3.6. Validation and real sample analyses: According to the previous reports [27, 28], a spectrophotometric method had been used for the determination of H₂O₂. This spectrophotometric method is based on the reaction of H₂O₂ with ammonium metavanadate in an acidic medium [27]. Here, the concentration of ammonium metavanadate is 8.0 mM and the concentration of sulphuric acid is 0.06 M. To obtain the maximum absorption of wavelength, UV-vis absorption spectra in the range of 350–800 nm were obtained for the mixture of H₂O₂/vanadate and compared with vanadate solutions. The strong absorption band at 450 nm is observed, indicating the formation of the peroxovanadium cation [27]. So, all the subsequent absorption measurements were conducted at 450 nm. As shown in Fig. 7, the absorbance of vanadate solution increased with the increasing of H₂O₂ concentration, and the linear curve was as shown in the inset; the analytical curve for peroxide was in the range 0.025–10.00 mM ($R = 0.9995$). In an attempt to explore the Mn₃O₄ OSMs/Nafion/GCE for application compared with the spectrophotometric method, two samples were measured by these two methods (Table 2). The recovery of H₂O₂ was determined by the standard addition method and the corresponding results are given in Table 2. One can see that the Mn₃O₄ OSMs/Nafion/GCE sensor also gives exact recovery ($\geq 95\%$). This result shows clearly the applicability of the Mn₃O₄ OSMs/Nafion/GCE in the determination of H₂O₂.

To test the potential use of the Mn₃O₄ OSMs/Nafion/GCE for analysis applications, a recovery experiment was conducted using the modified electrode in milk. The concentrations of hydrogen peroxide in milk samples were determined with the standard addition method. Three different concentrations of H₂O₂ were added under the optimal applied potential. All of the measurements were performed four times ($n = 4$), and the results are listed in Table 3. Acceptable recoveries and the relative standard deviation (RSD) were obtained, which indicates that the sensor developed in this work could be efficiently used for the determination of H₂O₂.

4. Conclusions: In summary, a non-enzymatic biosensor based on Mn₃O₄ OSMs was fabricated by the mixed solvothermal method. The Mn₃O₄ OSMs-modified electrode exhibited a high electrocatalytic activity for detecting H₂O₂. On the basis of the results, Mn₃O₄ OSMs have good electrocatalytic activity, rapid response and excellent stability, and therefore have great potential applications in the field of electrochemical sensors.

5. Acknowledgments: The authors thank the National Natural Science Foundation of China (nos. 21071005, 21271006), the Natural Science Foundation of the Anhui province of China (no. 1208085QE102), the Research Culture Funds of Anhui Normal University (nos. 2011rcpy038, 2014xmpy13), the Innovation Funds of Anhui Normal University (no. 2014cxjj13), the Natural Science Foundation of Anhui Higher Education Institutions of China (nos. KJ2013B305, KJ2010B250) and the Doctoral Research Initial Foundation of Wannan Medical College (no. 201221).

6 References

- [1] Liao K., Mao P., Li Y., *ET AL.*: 'A promising method for fabricating Ag nanoparticle modified nonenzyme hydrogen peroxide sensors', *Sens. Actuators B*, 2013, **181**, pp. 125–129
- [2] Narang J., Chauhan N., Pundir C.S.: 'A non-enzymatic sensor for hydrogen peroxide based on polyaniline, multiwalled carbon nanotubes and gold nanoparticles modified Au electrode', *Analyst*, 2011, **136**, pp. 4460–4466
- [3] Li W., Kuai L., Qin Q., Geng B.: 'Ag–Au bimetallic nanostructures: co-reduction synthesis and their component-dependent performance for enzyme-free H₂O₂ sensing', *J. Mater. Chem. A*, 2013, **1**, pp. 7111–7117
- [4] Wang J.: 'Carbon-nanotube based electrochemical biosensors: a review', *Electro Anal.*, 2005, **17**, pp. 7–14
- [5] Zhu H., Zhu Y., Yang X., Li C.: 'Multiwalled carbon nanotubes incorporated with dendrimer encapsulated with Pt nanoparticles: an attractive material for sensitive biosensors', *Chem. Lett.*, 2006, **35**, pp. 326–327
- [6] Xu J., Wei X.-W., Song X.-J., *ET AL.*: 'Synthesis and electrocatalytic activity of multi-walled carbon nanotubes/Cu–Ag nanocomposites', *J. Mater. Sci.*, 2007, **42**, pp. 6972–6976
- [7] Chen D., Feng H., Li J.: 'Graphene oxide: preparation, functionalization, and electrochemical applications', *Chem. Rev.*, 2012, **112**, pp. 6027–6053
- [8] Wu K.-L., Li X.-Z., Dong C., *ET AL.*: 'Enzyme-free amperometric H₂O₂ biosensor based on CU-AG bimetallic nanoparticles with reduced graphene oxide nanocomposites', *Chem. Lett.*, 2013, **42**, pp. 1466–1468
- [9] Zhang X., Zhang J., Zhou D., Wang G.: 'Electro deposition method to synthesise gold nanoparticles-Prussian blue-graphene

- nanocomposite and its application in electrochemical sensor for H_2O_2 ', *Micro Nano Lett.*, 2012, **7**, pp. 60–63
- [10] Cao G.S., Wang P., Li X., Wang Y., Wang G., Li J.: 'Hydrogen peroxide electrochemical sensor based on Fe_3O_4 nanoparticles', *Micro Nano Lett.*, 2014, **9**, pp. 16–18
- [11] Shanmugam S., Gedanken A.: 'MnO octahedral nanocrystals and MnO@C core-shell composites: synthesis, characterization, and electrocatalytic properties', *J. Phys. Chem. B*, 2006, **110**, pp. 24486–24491
- [12] Lima F.H.B., Calegari M.L., Ticianelli E.A.: 'Electro catalytic activity of manganese oxides prepared by thermal decomposition for oxygen reduction', *Electrochim. Acta*, 2007, **52**, pp. 3732–3738
- [13] Bai Y.-H., Xu J.-J., Chen H.-Y.: 'Selective sensing of cysteine on manganese dioxide nanowires and chitosan modified glassy carbon electrodes', *Biosens. Bioelectron.*, 2009, **24**, pp. 2985–2990
- [14] Xu J.-J., Luo X.-L., Du Y., Chen H.-Y.: 'Application of MnO_2 nanoparticles as an eliminator of ascorbate interference to amperometric glucose biosensors', *Electrochem. Commun.*, 2004, **6**, pp. 1169–1173
- [15] Feng J.-J., Zhang P.-P., Wang A.-J., Zhang Y., Dong W.-J., Chen J.-R.: 'One-pot hydrothermal synthesis of uniform β - MnO_2 nanorods for nitrite sensing', *J. Colloid Interface Sci.*, 2011, **359**, pp. 1–8
- [16] Bai Y.-H., Du Y., Xu J.-J., Chen H.-Y.: 'Choline biosensors based on a bi-electro catalytic property of MnO_2 nanoparticles modified electrodes to H_2O_2 ', *Electrochem. Commun.*, 2007, **9**, pp. 2611–2616
- [17] Wang A.-J., Zhang P.-P., Li Y.-F., Feng J.-J., Dong W.-J., Liu X.-Y.: 'Hydrogen peroxide sensor based on glassy carbon electrode modified with β -manganese dioxide nanorods', *Microchim. Acta*, 2011, **175**, pp. 31–37
- [18] Mohseni G., Negahdary M., Faramarzi H., ET AL.: 'Voltammetry behavior of modified carbon paste electrode with cytochrome C and Mn_2O_3 nanoparticles for hydrogen peroxide sensing', *Int. J. Electrochem. Sci.*, 2012, **7**, pp. 12098–12109
- [19] Gorlin Y., Chung C.-J., Nordlund D., Clemens B.M., Jaramillo T.F.: ' Mn_3O_4 supported on glassy carbon: an active non-precious metal catalyst for the oxygen reduction reaction', *ACS Catal.*, 2012, **2**, pp. 2687–2694
- [20] Gao M.-R., Xu Y.-F., Jiang J., Zheng Y.-R., Yu S.-H.: 'Water oxidation electro catalyzed by an efficient $Mn_3O_4/CoSe_2$ nanocomposite', *J. Am. Chem. Soc.*, 2012, **134**, pp. 2930–2933
- [21] Yin J., Gao F., Wu Y., Wang J., Lu Q.: 'Synthesis of Mn_3O_4 octahedrons and other manganese-based nanostructures through a simple and green route', *Cryst. Eng. Commun.*, 2010, **12**, pp. 3401–3403
- [22] Kamil Reza K., Singh N., Yadav S.K., Singh M.K., Biradar A.M.: 'Pearl shaped highly sensitive Mn_3O_4 nanocomposite interface for biosensor applications', *Biosens. Bioelectron.*, 2014, **62**, pp. 47–51
- [23] Si P., Dong X.-C., Chen P., Kim D.-H.: 'A hierarchically structured composite of $Mn_3O_4/3D$ graphene foam for flexible nonenzymatic biosensors', *J. Mater. Chem. B*, 2013, **1**, pp. 110–11
- [24] Liu S., Tian J., Wang L., Li H., Zhang Y., Sun X.: 'Stable aqueous dispersion of graphene nanosheets: noncovalent functionalization by a polymeric reducing agent and their subsequent decoration with Ag nanoparticles for enzymeless hydrogen peroxide detection', *Macromolecules*, 2010, **43**, pp. 10078–10083
- [25] Lu W., Liao F., Luo Y., Chang G., Sun X.: 'Hydrothermal synthesis of well-stable silver nanoparticles and their application for enzymeless hydrogen peroxide detection', *Electrochim. Acta*, 2011, **56**, pp. 2295–2298
- [26] Li L., Du Z., Liu S., ET AL.: 'A novel nonenzymatic hydrogen peroxide sensor based on MnO_2 /graphene oxide nanocomposite', *Talanta*, 2010, **82**, pp. 1637–1641
- [27] Nogueira P.R.F., Oliveira M.C., Paterlini W.C.: 'Simple and fast spectrophotometric determination of H_2O_2 in photo-Fenton reactions using metavanadate', *Talanta*, 2005, **66**, pp. 86–91
- [28] Harris D.C.: 'Quantitative chemical analysis' (W.H. Freeman, New York, 1999, 5th edn), p. 429